



HAL
open science

**On the peculiar torque reversals and the X-ray
luminosity history of the accretion-powered X-ray pulsar
4U 1626–67**

Onur Benli

► **To cite this version:**

Onur Benli. On the peculiar torque reversals and the X-ray luminosity history of the accretion-powered X-ray pulsar 4U 1626–67. *Monthly Notices of the Royal Astronomical Society*, 2020, 495 (4), pp.3531-3537. 10.1093/mnras/staa998 . hal-02491273

HAL Id: hal-02491273

<https://hal.science/hal-02491273v1>

Submitted on 23 May 2024

HAL is a multi-disciplinary open access archive for the deposit and dissemination of scientific research documents, whether they are published or not. The documents may come from teaching and research institutions in France or abroad, or from public or private research centers.

L'archive ouverte pluridisciplinaire **HAL**, est destinée au dépôt et à la diffusion de documents scientifiques de niveau recherche, publiés ou non, émanant des établissements d'enseignement et de recherche français ou étrangers, des laboratoires publics ou privés.

On the peculiar torque reversals and the X-ray luminosity history of the accretion-powered X-ray pulsar 4U 1626–67

O. Benli ^{1,2}★

¹*Department of Physics and Astronomy, Southampton University, Southampton SO17 1BJ, UK*

²*Observatoire Astronomique de Strasbourg, 11 rue de l'Université, 67000 Strasbourg, France*

Accepted 2020 April 6. Received 2020 April 6; in original form 2020 February 9

ABSTRACT

The X-ray luminosity (L_x) and the rotational properties of 4U 1626–67 have been measured at regular intervals during the last four decades. It has been recorded that the source underwent torque reversals twice. We have tried to understand whether these eccentric sign-switches of the spin period derivative (\dot{P}) of 4U 1626–67 could be accounted for with the existing torque models. We have found that the observed source properties are better estimated with the distances close to the lower limit of the previously predicted distance range (5–13 kpc). Furthermore, assuming an inclined rotator, we have considered the partial accretion/ejection from the inner disc radius that leads to different L_x – \dot{P} profiles than the aligned rotator cases. We have concluded that the oblique rotator assumption with the inclination angle $\chi \sim (10^\circ\text{--}30^\circ)$ brings at least equally best fitting to the observed L_x and \dot{P} of 4U 1626–67. More importantly, the estimated change of the mass accretion rate, which causes the change in observed L_x of 4U 1626–67 is much less than that is found in an aligned rotator case. In other words, without the need for a substantial modification of mass accretion rate from the companion star, the range of the observed L_x could be explained naturally with an inclined magnetic axis and rotation axis of the neutron star.

Key words: accretion, accretion discs – stars: individual: 4U 1626–67 – X-rays: binaries.

1 INTRODUCTION

In accreting X-ray binaries where the period change of compact star is observed to be steady and persistent, the accretion on to star is thought to occur along with the disc. Low-mass X-ray binaries (LMXBs) are good examples of those kinds of systems. On the other hand, in the high-mass X-ray binaries (HMXBs), the mass accretion is fed mostly by the wind from the companion star. In such a wind-fed accreting system, period derivative varies in short time-scales because of the quick alternation of accretion geometry and variation in the amount of matter being accreted. Also, short but steady episodes of spin-change observed from some wind-fed systems, are indicative of the formation of the short-duration transient accretion discs in these systems.

Some accretion powered X-ray pulsars have shown fascinating torque reversals separated by time-scales from weeks to months while for some systems, this time-scale can be as much as a few decades. The X-ray pulsar 4U 1626–67 in an LMXB was first observed by *Uhuru* (Giacconi et al. 1972). The pulsar with the spin period $P \simeq 7.6$ s (Rappaport et al. 1977), was confirmed to reside in an ultracompact binary system with a very low mass

companion with the estimated mass in the $\sim 0.03\text{--}0.09 M_\odot$ range. The actual mass of the companion varies depending on the binary inclination angle $11^\circ \leq i \leq 36^\circ$ (Levine et al. 1988; Chakrabarty et al. 1997). An optical counterpart, KZ TrA, was subsequently detected by McClintock et al. (1977). Pulsed optical emission, which was attributed to reprocessing of pulsed X-rays from the surface of the companion, revealed the 42 min orbital period of the binary (Middleditch et al. 1981; Chakrabarty 1998). The existence of an accretion disc around 4U 1626–67 has been well established via particularly double-peaked emission lines in the X-ray band (Schulz et al. 2001).

The torque history of 4U 1626–67 was reviewed in detail by Camero-Arranz et al. (2010). For the recent spectral and timing analysis of the source, we refer to Iwakiri et al. (2019). The persistent X-ray pulsar that has been monitored several times since its discovery underwent two torque reversals on 1990 June (Chakrabarty et al. 1997) and 2008 February (Camero-Arranz et al. 2010). The source was steadily spinning-up (SU) with the period derivative $\dot{P} \sim 10^{-10} \text{ s s}^{-1}$ and the X-ray luminosity $L_x \sim 10^{37} \text{ erg s}^{-1}$ before its transition to the spin-down (SD) phase in 1990. Interestingly, the source was spinning down with a similar rate to the pre-reversal SU rate. Subsequently, the source was observed many times in the steady SD phase for 18 years until the second torque reversal occurred in 2008, switching again to the SU phase.

* E-mail: onorbenli@sabanciuniv.edu

The elaborated observations of 4U 1626–67 indicate that the torques acting on the neutron star and the X-ray luminosity are related to each other in most cases. The source was able to monitor in the course of the latter reversal. On the contrary, there was no observation during the first reversal. However, observation of the source in 1991 revealed that the pulsar started to SD, which confirmed the sign change of the pulsar's \dot{P} . Camero-Arranz et al. (2010) showed that the X-ray flux of the source in 2010, two years after the torque reversal in 2008, has reached up almost the same level as in 1977. The 2008 reversal occurred at a similar but slightly lower X-ray luminosity level compared to the 1990 reversal.

Chakrabarty et al. (1997) estimated that the mass accretion rate on to the star is supposed to be greater than $4 \times 10^{16} \text{ g s}^{-1}$ ($2 \times 10^{-10} M_{\odot} \text{ yr}^{-1}$) for the observed period derivative, $\dot{P} = -6.5 \times 10^{-12} \text{ s s}^{-1}$ ($\dot{\nu} = 8.5 \times 10^{-13} \text{ Hz s}^{-1}$) at that time. Chakrabarty (1998) favoured an X-ray irradiated accretion disc over the radiatively driven wind accretion and showed that irradiated disc calculation provides a better fit to the optical photometry.

Much longer spin-up time-scales of Cen X-3 and Her X-1, compared to those of other accreting systems, were not in line with the initiative models proposed to explain spin behaviour of accreting pulsars (Rappaport & Joss 1977; Ghosh & Lamb 1979). Cen X-3 and Her X-1 also showed short-term SD behaviour interspersed among their spin-up epochs. The X-ray luminosity of these sources did not vary significantly during transitions indicating that the sources continued to accrete while the torque acting on the sources was observed to change its sign. Therefore, the X-ray luminosity and torque variations of Cen X-3 and Her X-1 have not been matching with the prediction of existing accretion models so far.

We tested here whether the X-ray luminosity and the torque (\dot{P}) history of 4U 1626–67 recorded in the last ~ 40 yr could be reproduced by the different regimes in the accretion-disc torques. We aimed to account for the L_x and the \dot{P} of the source by considering the simultaneous effect of the spin-up and the SD torques acting on the star by an accretion disc as well as taking into account oblique rotator effects. We employed two different torque models and implemented the inclination of the magnetic axis of the star to its rotation axis into one of these models. In Section 2, we describe the models. The results are presented in Section 3. We discuss the implication of our results in Section 4.

2 ACCRETION ON TO MAGNETIZED STAR

In a Keplerian accretion disc, the angular velocity of the falling matter, Ω_K , increases as it becomes closer to the star. At the corotation radius, Ω_K is equivalent to the angular velocity of the star, $\Omega_K(r_{\text{co}}) = \Omega_*$ which can be written as

$$r_{\text{co}} = \left(\frac{GM}{\Omega_*^2} \right)^{1/3} = \left(\frac{GMP^2}{4\pi^2} \right)^{1/3}. \quad (1)$$

The inner radius of the accretion disc, r_{in} , is usually expressed as a fraction of the conventional Alfvén radius

$$r_A = \left(\frac{\mu^2}{\sqrt{2GM\dot{M}}} \right)^{2/7}, \quad (2)$$

where M and μ are the mass and magnetic dipole moment of the star, G the gravitational constant and \dot{M} the mass inflow rate at that radius. In the propeller phase, the realistic inner disc radius where viscously inflowing disc truncated by the dipole field of the star is expected to be close to r_A . In literature, the relation $r_{\text{in}} = (0.5-1) r_A$ has been widely used to define r_{in} . The actual location of r_{in} is dependent on the details of disc field interaction (Ghosh & Lamb

1979; Arons 1993). Some authors assume that the critical value of r_A , below which accretion on to star is expected to be switched-on, is determined by the light cylinder radius $r_{\text{LC}} = c/\Omega_*$. When $r_A < r_{\text{LC}}$, the system is assumed to be in the accretion, where the disc matter arriving at r_{in} flows on to the star. However, the observed rotational properties and X-ray luminosity of transitional millisecond pulsars contradict with the condition that r_A has to be closer or larger than r_{LC} to switch-off accretion on to the star (Archibald et al. 2015; Papitto & Torres 2015; Ertan 2017).

In the accretion phase, the X-ray luminosity of the neutron star is calculated by

$$L_X = \frac{GM\dot{M}_{\text{acc}}}{R}, \quad (3)$$

where \dot{M}_{acc} is the mass accretion rate on to the star, and R is the radius of the star. Accretion on to neutron star through a prograde disc makes the star spinning faster. Because the angular momentum of matter coupled to dipole field lines is superimposed over that of the star. Even if the total mass of the accreted matter is negligible about the mass of the star. In other words, the neutron star spins up due to the torque by the material being accreted (Pringle & Rees 1972),

$$\Gamma_{\text{SU}} = \dot{M}_{\text{acc}} \sqrt{GM r_{\text{in}}}. \quad (4)$$

In addition to the spin-up material torque, SD torque also acts on the star due to the interaction between the dipole field and plasma in the disc (Ghosh & Lamb 1979; Wang 1995; Erkut & Alpar 2004, 2008; Rappaport, Fregeau & Spruit 2004). The total torque acting on the star is

$$\Gamma_{\text{TOT}} = \Gamma_{\text{SU}} + \Gamma_{\text{SD}}. \quad (5)$$

There exist several different approaches to interpret Γ_{SD} that will be the main discussion in the following sections. The total torque can also be written as

$$\dot{P} = -\frac{p^2}{2\pi I} \Gamma_{\text{TOT}}, \quad (6)$$

where I is the moment of inertia of the star. We assume that the conventional moment of inertia of a neutron star is $I = 10^{45} \text{ g cm}^2$ throughout this work, since considering I as a free parameter does not provide any constraint to theoretical models apart from a systematic shift in \dot{P} prediction.

2.1 Model I

Earlier theoretical models imply that neutron stars with conventional dipole field strengths could be in the fast-rotator phase while at the same time continue to accrete matter from the disc [e.g. (Rappaport et al. 2004)]. The star is thought to be in the propeller SD state for $r_A > r_{\text{co}}$ as the in-flowing disc matter is expelled from the system by the rotating magnetic field lines (Illarionov & Sunyaev 1975). Ertan (2017) set forth the condition that the magnetic torque acting on the in-flowing matter has to accelerate it to the speed of the field lines within the interaction time-scale in order to sustain a steady propeller. This condition leads that the star can accrete when $r_{\text{in}} \sim r_{\text{co}}$ even for $r_A \gg r_{\text{co}}$.

In the case that disc-magnetosphere interaction occurs along a narrow boundary region, assuming the strength of the dipole field does not change significantly through the boundary, the SD torque acting on the star by the disc can be written as (Ertan 2018)

$$\Gamma_{\text{SD},1} = -\frac{\mu^2}{r_{\text{in}}^3} \left(\frac{\Delta r}{r_{\text{in}}} \right), \quad (7)$$

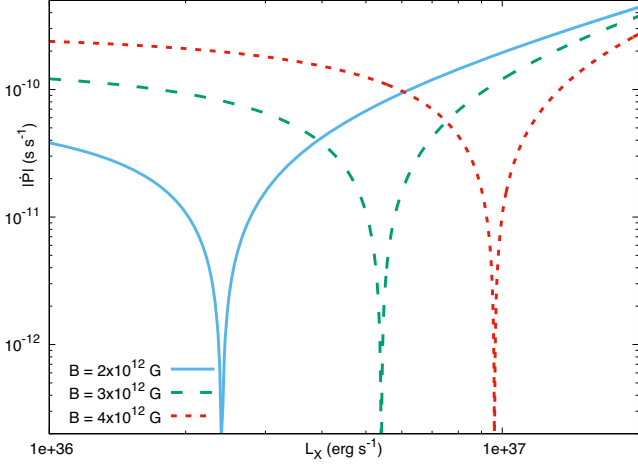


Figure 1. Illustrative model curves indicating the change of the magnitude of \dot{P} by \dot{M} for three different magnetic field strengths given in the bottom left corner. The curves are produced by using equation (9) for the SD torque. The critical L_x for the torque reversal is determined by B .

where Δr is a free parameter denoting the boundary width of the disc-magnetosphere interaction region and μ is the magnetic dipole moment of the neutron star. The strength of the dipole field on the surface of the star is $B = \mu/R^3$.

Since observations imply that the source 4U 1626–67 has always been in the accretion phase, we take $r_{\text{in}} = r_{\text{co}}$ in our calculations. Regarding the observed L_x interval of 4U 1626–67, r_{in} is expected to be extending down to r_{co} (Ertan 2017, 2018). We assume all of the matter arriving at the inner disc flows on to the star. Adopting $M = 1.4 M_{\odot}$, the X-ray luminosity is found by equation (3) for all three models in this work (Model I, Model II, and the Model II + oblique rotator). However, we calculate \dot{M} via numerical integration along the azimuthal angle for the oblique rotator case (see Section 2.3). We should note that the total torque acting on the star can be negative or positive while the system is always in the accretion phase for all models in this work.

It can be seen in equation (7) that the SD torque only depends on the magnetic field strength of the star and the parameter Δr associated with the width of the interaction region between the magnetic field of the star and disc. Therefore, the transition luminosity (or the critical \dot{M}) is unique for a given B and fixed Δr . We adopt a constant Δr for all \dot{M} in a model curve. $\Gamma_{\text{SD},1}$ has similar trend to $\Gamma_{\text{SD},2}$ (equation 9) while it is slightly less efficient compared to $\Gamma_{\text{SD},2}$. The sample model curves found by adopting $\Gamma_{\text{SD},2}$ for the SD torque for different B values are presented in Fig. 1.

2.2 Model II

The SD disc torque acting on the neutron star can also be found by integrating the magnetic torque from r_A to r_{co} (Erkut & Alpar 2004),

$$\Gamma_{\text{SD},2} \simeq - \int_{r_{\text{co}}}^{r_A} r^2 B_{\phi}^+ B_z dr, \quad (8)$$

where $B_z \simeq -\mu/r^3$ is the z-component of the dipolar magnetic field of the neutron star in the cylindrical coordinates. $B_{\phi}^+ = \gamma_{\phi} B_z$ is the azimuthal component of the magnetic field on the surface of the disc and γ_{ϕ} denotes the azimuthal pitch. Due to the very sharp radial dependence of the magnetic pressure, most of the contribution to the SD torque comes from the radii close to r_{co} . In this case, taking

$\gamma_{\phi} = 3/2$, after the integration of (8), we have

$$\Gamma_{\text{SD},2} = \frac{1}{2} \dot{M}_{\text{in}} (GM r_A)^{1/2} (1 - \omega_*^2) \quad (9)$$

(see Ertan & Erkut 2008 for model description in detail), where \dot{M}_{in} is the rate of the mass inflow at r_{in} and ω_* is the fastness parameter defined by the ratio of r_A to r_{co} , $\omega_* = (r_A/r_{\text{co}})^{3/2}$. It should be noted that the critical fastness parameter, above which accretion is expected to be halted, is still controversial.

We would like to draw attention to that in the accretion phase, $\Gamma_{\text{SD},2}$ described in equation (9), does not depend on \dot{M}_{in} (similar to $\Gamma_{\text{SD},1}$). In other words, SD torque is constant in the accretion phase since, the \dot{M} dependence of r_A , hence ω_* , leaves $\Gamma_{\text{SD},2}$ independent of \dot{M} in the accretion phase. The spin-up torque acting on the star, due to the angular momentum of the matter being accreted (equation 4) causes varying total torque by \dot{M}_{in} . There exists a particular regime where SU and SD torques are comparable. In this regime, the system enters into, e.g. the transition from the SD phase to SU phase with increasing \dot{M}_{in} . The total torque decreases but the star is still in the SD regime until \dot{M}_{in} reaches the critical value. The total torque acting on the star switches sign; thus, the system makes a transition to the SU phase. Likewise, the reverse transition can take place from the SU phase to the SD phase with decreasing \dot{M}_{in} .

Given that 4U 1626–67 has always been in the accretion phase, and P has not been significantly changed since its discovery,

$$\dot{P} \simeq A + \frac{B}{L_x} \quad (10)$$

can be found from equation (1) and equations (3)–(6) where $A = -P^2 \Gamma_{\text{SD}} (2\pi I)^{-1}$ and $B = -(P)^{7/3} (2\pi)^{-4/3} (GM)^{5/3} (RI)^{-1}$ are invariants for the constants, G , M , R , and B (so Γ_{SD} is also constant). The former and latter terms denote the effects of SD and spin-up torques, where only Γ_{SD} is distinct for Model I and Model II. We should note that equation (10) can not be used for the oblique rotator case because the mass accretion rate is calculated by integration along the azimuthal angle in this case which means $\dot{M}_{\text{acc}} \leq \dot{M}_{\text{in}}$ depending on the inclination angle. In Fig. 1, we show three model curves with different field strengths to indicate that the critical L_x where \dot{P} changes its sign strongly depends on the value of the magnetic field. The critical \dot{M} (or L_x) is found to be larger for stronger dipole fields in both Model I and Model II. It can be useful to emphasize that the similar regime where \dot{P} changes sign while the star carries on accreting matter exists in the same way for the Model I described in Section 2.1.

So far, we have been dealing with the aligned rotator cases, where the magnetic axis of the neutron star is parallel to its rotation axis. In the following section, we present a description of the model for a non-aligned configuration.

2.3 Model II + oblique rotator

Perna, Bozzo & Stella (2006) investigated the interaction between magnetosphere and disc for an oblique rotator (the angle between the spin axis of the pulsar and the disc plane is $\chi \neq 0$). The authors supposed that the material torque dominates the total torque; however, they did not take into account the magnetic SD torque through the disc-magnetosphere boundary. Here, we additionally calculate the effect of SD torques but do not consider the re-joining of the ejected matter into the outer disc for the sake of simplicity. Perna et al. (2006) predicted that, even if the mass supply from companion to the accretion disc is constant, cyclic transitions

Table 1. The bolometric X-ray flux and the period derivative of 4U 1626–67 measured at different times since 1978. See table 1 in Takagi et al. (2016) for the references.

Date	F_{bol} ($10^{-10} \text{ s}^{-1} \text{ cm}^{-1}$)	\dot{P} ($10^{-11} \text{ s s}^{-1}$)
1978 Mar	25 ± 3	-4.55
1979 Feb	19 ± 1	-4.9 ± 0.1
1983 May	19.0 ± 0.4	-13 ± 5
1983 Aug	20.3 ± 1.8	-5.65 ± 0.10
1986 Mar	22 ± 0.7	-4.96 ± 0.06
2001 Aug	6.3	3.39 ± 0.96
2003 Jun	6.3	2.74 ± 0.37
2003 Aug	5.6	4.6 ± 1.2
2007 Jun	5.6 ± 0.2	2.9
2007 Sep	5.2 ± 0.2	2.7
2007 Dec	8.0 ± 0.3	1.9
2008 Jan	9.3 ± 0.4	0.18
2008 Feb	11.5 ± 0.3	-0.53
2008 Mar	14.5 ± 0.3	-2.3
2008 Jun	14.8 ± 0.2	-2.7

between the SU phase and the SD phase can be realized for larger inclination angles than a critical angle.

In cylindrical coordinates, the magnetic dipole field of an oblique rotator can be defined by

$$B^2 = \frac{\mu^2}{r^6} [1 + 3(\sin \chi \sin \phi)^2] \quad (11)$$

(Jetzer, Strässle & Straumann 1998; Campana et al. 2001) which leads magnetospheric radii of the elliptical form in the disc plane

$$r_M(\phi) = r_A [1 + 3(\sin \chi \sin \phi)^2], \quad (12)$$

where ϕ is the azimuthal angle. In the co-rotating magnetosphere of the star, Kelvin–Helmholtz instability enables the material in the Keplerian disc to fill the empty regions within a short time-scales enough (Perna et al. 2006). The inner disc can therefore remain in steady contact with the magnetosphere. The speed of the field lines should be higher than the local escape velocity, i.e. $r_{\text{in}} > 1.26 r_{\text{co}}$, to enable the ejection of disc material (at r_{in}) from the system by propeller mechanism.

In the oblique rotator case, as the inner disc radius $r_M(\phi)$ is different at each angle ϕ , the system could be in the partial propeller regime. In other words, some azimuthal angles lead the matter arriving at r_M at those angles to be ejected out of the system while at the other angles, all the in-flowing matter accrete on the star. We should therefore calculate the mass accretion rate on to the star for each angle, separately and the integration from 0 to 2π gives the total rate of the mass accretion on to the star (\dot{M}_{acc}). This partly accreting/propelling system could cause strong variation in L_x even though the mass supply from the companion (\dot{M}) does not change significantly (see Table 2). We should note that, for the aligned rotator cases (Model I and Model II), the rate of mass supplied from the companion is equal to the rate of the mass accrete on to the star, i.e. $\dot{M} = \dot{M}_{\text{acc}}$.

To take into account the effect of an inclined rotator, we employ a simple two-dimensional model involving the disc torques braking the star. Along the azimuthal angle grid, $\phi + \Delta\phi$, we integrate the amount of mass accreted and SU-material-torque and SD-disc-torque while assuming that all the incoming disc material is ejected for $r_M > r_{\text{co}}$. We implement the oblique case into Model II, where disc torques are integrated from r_{co} to r_A to compare with our predictions for the aligned magnetic and rotation axis of the star.

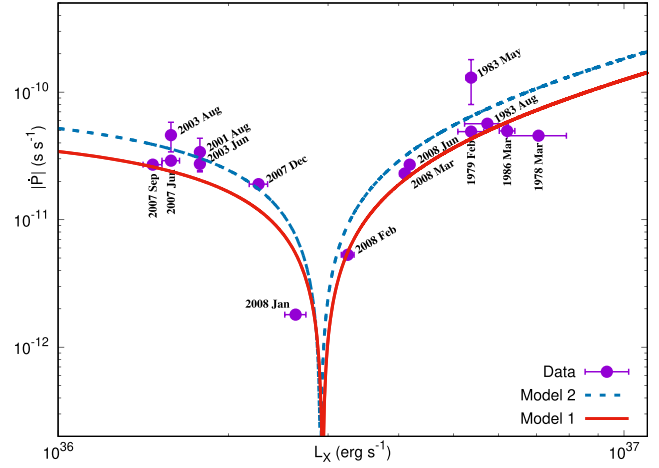


Figure 2. Two model curves qualitatively fitting to the observed L_x and \dot{P} data of 4U 1626–67 for $d = 5$ kpc, $M = 1.4 M_{\odot}$ and $R = 10$ km. The data points with error bars (see Table 1) indicate the observed values where L_x is the bolometric luminosity. The dashed (blue) curve is calculated by Model II with $B = 2.2 \times 10^{12}$ G. The solid (red) curve is calculated by Model I with $\Delta r/r_{\text{in}} = 0.15$ and $B = 3.2 \times 10^{12}$ G.

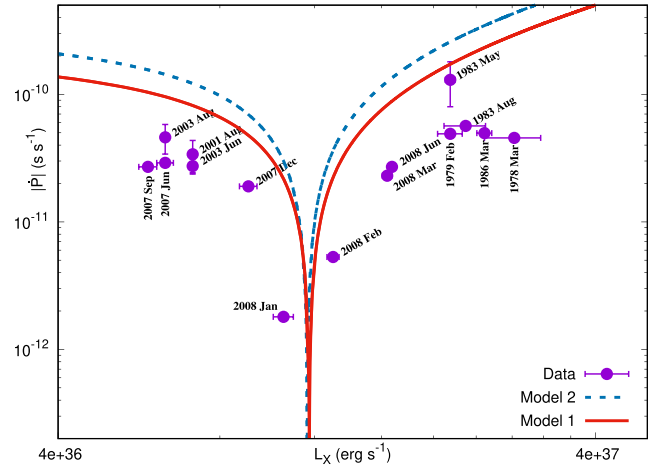


Figure 3. Two illustrative model curves for comparing the observed L_x (for $d = 10$ kpc) and \dot{P} data of 4U 1626–67, with $M = 1.4 M_{\odot}$ and $R = 10$ km. The dashed (blue) curve is calculated by Model II with $B = 4.4 \times 10^{12}$ G. The solid (red) curve is calculated by Model I with $\Delta r/r_{\text{in}} = 0.15$ and $B = 6.4 \times 10^{12}$ G. The predictions of the models are not consistent with the observed properties of the source for large distances.

3 RESULTS

We investigated the torque and X-ray luminosity measurements of 4U 1626–67 performed at various time intervals for ~ 40 yr, considering three different torque models (Model I, Model II, and Model II + oblique rotator). We adopted the data presented by in Table 1. The X-ray fluxes were converted into (0.5–100) keV energy band by Takagi et al. (2016) with the spectral model in Camero-Arranz et al. (2012). We examined the L_x and \dot{P} observations in both spin-up and SD phases of the aligned rotator assumptions. Figs 2 and 3 show our results for the aligned rotator, for the distances $d = 5$ kpc and $d = 10$ kpc. We presented the results for the oblique case in Fig. 4. In all our calculations, we adopted the conventional mass and radius of neutron star, $M = 1.4 M_{\odot}$ and $R = 10$ km. Within the possible

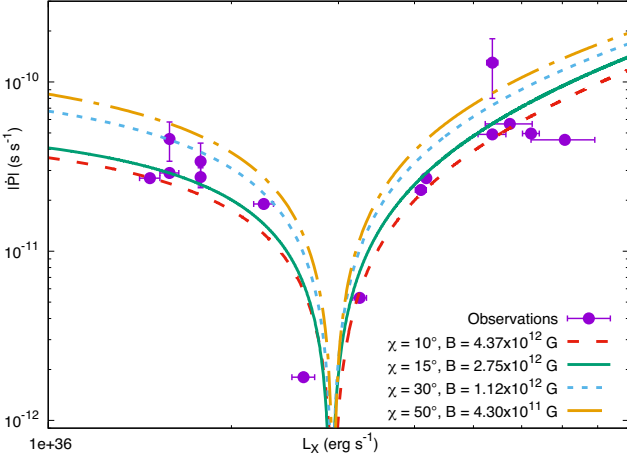


Figure 4. The model curves for different angles between the rotation axis and the magnetic axis, χ , with the field strengths given in the bottom right of the figure. There is a unique B value for each χ which could result in the torque reversing at the same critical L_x . The observed data is the same to Figs 2–3. We do not show the labels of data to avoid the overlap of the labels and curves.

Table 2. The required amount of change in \dot{M} for a three-fold increase in L_x for the model curves presented in Fig. 4. Each line represents the different angles between the rotation axis and the magnetic axis. \dot{M}_1 and \dot{M}_2 are the mass accretion rates which give $L_x = 2 \times 10^{36} \text{ erg s}^{-1}$ and $L_x = 6 \times 10^{36} \text{ erg s}^{-1}$. The magnetic field strengths that could produce each model curve is listed in the last column.

	$\dot{M}_1 \text{ (g s}^{-1}\text{)}$	$\dot{M}_2 \text{ (g s}^{-1}\text{)}$	$B \text{ (G)}$
$\chi = 10^\circ$	1.97×10^{17}	2.00×10^{17}	4.37×10^{12}
$\chi = 15^\circ$	8.02×10^{16}	9.34×10^{16}	2.75×10^{12}
$\chi = 30^\circ$	2.79×10^{16}	5.32×10^{16}	1.12×10^{12}
$\chi = 50^\circ$	2.00×10^{16}	4.40×10^{16}	4.30×10^{11}

range of the source distance, 5–13 kpc (Chakrabarty 1998; Takagi et al. 2016), we tried different distances to fit the data and found that the lowest distance, $d = 5$ kpc, produces the best model curves. We also present our results for $d = 10$ kpc in order to indicate that fitting quality decreases for larger distances.

The solid and dashed lines in Figs 2 and 3 are produced by employing Model I and Model II, respectively. The data points with error bars indicate the L_x and \dot{P} measurements for the years presented next to the data points on the figures. The dips appearing in the $\dot{P} - L_x$ curves remark the transition luminosity. The left-hand side of the dip corresponds to the SD phase with a positive \dot{P} . As seen in Fig. 2, the observed data on the left-hand side of the dip can be produced better with Model II while that is on the right-hand side with Model I, for $d = 5$ kpc. For higher luminosities on the right-hand side of the dip, the source is in the SU phase. The \dot{P} reverses its sign at the most bottom of the dip which is not seen on the figures. We would like to point out that the two data points, 2008 January and 2008 February, were measured when the source was in the torque reversal epoch. These two data points determine the transition location and constrain the width of the dip and hence enable us to pin down the B values for a given distance.

In Fig. 2, the observed L_x and \dot{P} of 4U 1626–67 are produced with the dipole field strengths $B = 2.2 \times 10^{12} \text{ G}$ and $B = 3.2 \times 10^{12} \text{ G}$ by using the Model II and the Model I. The Model I curve is found with $\Delta r/r_{\text{in}} = 0.15$. The less efficient torque, $\Gamma_{\text{SD},1}$ (equation 7),

could better account for the two data point during the transition in 2008 and the data in the spin-up phase, while $\Gamma_{\text{SD},2}$ could fit the data better in the SD phase.

Employing $\Gamma_{\text{SD},2}$ found through integrating disc torques from r_{co} to r_A and assuming an oblique rotator for the star, we found the similar $\dot{P} - L_x$ curves producing the observed $\dot{P} - L_x$ of 4U 1626–67. However, depending on the angle between the magnetic axis and rotation axis, we estimated different magnetic field strengths of the star. We present the model results in Fig. 4 and Table 2. We found that the best result consistent with the observed properties of 4U 1626–67 could be found with $\chi \sim 15$ and $B = (2-3) \times 10^{12} \text{ G}$ for $d = 5$ kpc. For this parameters, the system is found to be in such an interesting regime that a small increase in \dot{M} leads a substantial change in L_x , e.g. $L_x = 2 \times 10^{36} \text{ erg s}^{-1}$ is produced with $\dot{M} \simeq 8 \times 10^{16} \text{ g s}^{-1}$ while $\dot{M} \simeq 9.3 \times 10^{16} \text{ g s}^{-1}$ gives $L_x = 6 \times 10^{36} \text{ erg s}^{-1}$. Therefore, the observed range of L_x from 4U 1626–67 does not require a significant change of mass accretion rate from the companion in this model.

Again in the oblique rotator case, similar to the aligned rotator models, the left- and right-hand sides of the reversal point (see Fig. 4), the best fitting model curves are produced with different χ values. For instance, the model curve with $\chi = 10^\circ$ better fit the data in the SU phase while $\chi \sim (15^\circ - 30^\circ)$ provide better model curves for the data in the SD phase.

4 DISCUSSION AND CONCLUSION

The cyclotron line feature of 4U 1626–67 at $\sim 37 \text{ keV}$ indicates that the strength of the magnetic dipole field is $B \simeq 3 \times 10^{12} \text{ G}$ at the surface of the star (Orlandini et al. 1998; D’Aì et al. 2017). A significant change in cyclotron line energy did not accompany the torque reversal while X-ray flux increased a factor of ~ 3 (Camero-Arranz et al. 2012) albeit the shape of pulse profile radically changed which was interpreted as the emission from accretion column switched from a pencil-beam to a fan-beam pattern (Koliopanos & Gilfanov 2016). Also employing the beat frequency model, Orlandini et al. (1998) estimated that the magnetic field is $B \sim (2-6) \times 10^{12} \text{ G}$, comparable to the field strength indicated by the cyclotron line feature. The model curves that we showed to be good candidates to account for the observed \dot{P} and L_x of the source are produced with $B \simeq (2-3) \times 10^{12} \text{ G}$ that is in line with those predictions.

Iwakiri et al. (2019) performed energy-resolved pulse profile analysis of 4U 1626–67 and could infer the inclination angle between the magnetic axis and rotation axis of the star. As the model used by Iwakiri et al. (2019) incorporates antisymmetric magnetic poles, a direct comparison of the prediction of our simple model ($\chi \sim 15^\circ$) with their estimation, is not straightforward. With an optimistic point of view to find a match between the prediction of our results and that of Iwakiri et al. (2019), the best-fitting value for the longitude of the first accretion column found by Iwakiri et al. (2019), 12° , does not contradict with the reasonable range of the obliquity that we found here.

One of the most intriguing features of the sources that underwent torque reversing is that the magnitude of the torque is similar while the sign of the torque reverses. What can be the physical mechanism responsible for this cabalistic behaviour is still an open question. According to our results, this could be the result of observational selection effect such that the sharp change of \dot{P} , when \dot{M} is close to the critical mass accretion rate, could make \dot{P} harder to observe within this range. However, as the magnitude of \dot{P} decreases sufficiently when \dot{M} is far from the SU/SD transition

point, measuring \dot{P} in both SU and SD phases is more likely for the source far from the transition. That is to say, the limiting conditions above could be one possibility why $|\dot{P}|$ is in the same order in both phases.

The models that are built upon the disc torque via interaction by the dipole field lines require fine-tuned alternation of the mass accretion rates to reproduce the observed torques of similar magnitude but with opposite signs. Makishima et al. (1988) proposed the idea that the SU–SD transition of GX 1+4 might be caused by the disappearance of the prograde disc and subsequent formation of the wind-fed retrograde disc. The alternations in the rotation direction of the discs could lead the torques with different signs but similar magnitudes. The models developed upon the retrograde disc suggestion could explain the inverse proportionality of the X-ray luminosity and spin-up torque as well as the positive correlation of SD torque and the X-ray luminosity of GX 1+4 (Chakrabarty et al. 1997; Nelson et al. 1997). It is, however, unlikely that Roche lobe overflow accretion can result in a retrograde disc. Unlike GX 1+4, 4U 1626–67 has a very low mass companion. Therefore, imposing retrograde accretion disc is inconvenient to explain the observed torque inversion of 4U 1626–67.

During the SD phase of 4U 1626–67, Chakrabarty (1998) detected 48 mHz quasi-periodic oscillation (QPO) in both X-ray and optical bands. Raman et al. (2016) analysed the 2014 data of the source and detected a weak ~ 48 mHz optical QPO but could not detect any QPO in the corresponding X-ray data. The QPO frequency is thought to be associated with the angular velocity of the pulsar and Keplerian angular velocity at the inner disc as such in the beat frequency model, $\omega = \Omega_K(r_{\text{in}}) - \Omega_*$ (Alpar & Shaham 1985). Therefore, investigating the evolution of the QPO frequency of accreting sources with varying mass accretion rates is of great importance to trace the actual mass accretion rate. Correct determination of the accretion rate is essential in order to obtain a proper torque model accounting for the strange L_x and torque behaviours.

The SD of the star could occur via disc-magnetosphere interaction beyond r_{co} (Ghosh & Lamb 1979; Wang 1995; Rappaport et al. 2004) or the mass ejection from the system by winds could extract angular momentum from the star and cause the slow-down (Arons & Lea 1980). In the Ghosh–Lamb type of models, the spin-up torque and SD torque expressed as a single term involving the dimensionless torque, which depends on the fastness parameter ω_* . The evolution of the system is accompanied by continuous change in ω_* . When ω_* is equal to the critical value $\omega_{*,c}$, the torque acting on the star vanishes and the system undergoes the torque reversal. Regarding that the observed QPO frequency of 4U 1626–67 is due to magnetospheric beat-frequency in the spin-up phase before the 1990 reversal, Vaughan & Kitamoto (1997) found that the Ghosh & Lamb (1979) model implies $\omega_{*,c} = 0.95$. Although ω_* , in none of the models we have used here, meets the same meaning as in Ghosh & Lamb (1979) (we have assumed $r_{\text{in}} = r_{\text{co}}$), yet it may be good to mention. The results of Model I and Model II (Fig. 2) manifest $\omega_{*,c} = 2.25$ and $\omega_{*,c} = 1.64$ while the oblique rotator calculations with $\chi = 10^\circ$, $\chi = 15^\circ$, $\chi = 30^\circ$, and $\chi = 50^\circ$ (Fig. 4) indicate $\omega_{*,c} = 0.99$, $\omega_{*,c} = 0.97$, $\omega_{*,c} = 0.65$, and $\omega_{*,c} = 0.32$. See also Vasilopoulos et al. (2020), Parfrey, Spitkovsky & Beloborodov (2016) for the estimation of $\omega_{*,c}$ in different models.

Vaughan & Kitamoto (1997) discussed that the observations of the source across the transition from the SU phase to the SD phase indicate that the QPO frequency increased from 40 to 48 mHz. This increase in the QPO frequency raised difficulties for magnetospheric beat-frequency model as the origin of QPO frequency. Türkoğlu

et al. (2017) used a fictitious polynomial for the torque to fit the X-ray data of 4U 1626–67 during the 2008 reversal and found that the torque has a cubic dependence on the fastness parameter near the torque equilibrium.

We did not attempt here to explain the properties of 4U 1626–67 during the torque reversals which will be studied in a separate work including the modelling of the evolution of the X-ray luminosity and torque in the SU phase and the SD phase of the source. Nevertheless, we would like to touch briefly on the rise of the X-ray flux during the 2008 reversal, which is not the case for the 1990 reversal. In the models we utilized here, the transition occurs smoothly rather than the abrupt change in the X-ray flux. If the rate of the mass accretion is modulated by instability at the interaction region of disc-magnetosphere, this could cause a fast variation of L_x .

Also, we would like to point out that we do not take into account the case $r_{\text{in}} < r_{\text{co}}$ which would lead a disc torque SU the star contrary to disc torques we adopted in this work which always slows down the star. In our model, the star makes the transition as the domination between the disc torque or the material torque reverses. Therefore, our model implies that an enhancement of mass accretion rate (e.g. due to thermal-viscous instability in the disc) occurred somehow before the 2008 reversal and took the mass accretion rate above the critical value, where the system switched into the spin-up phase. The change of the pulse profile of 4U 1626–67 during the transitions (Krauss et al. 2007; Beri et al. 2014) might be indicative of a sharp change in the rate of the mass accretion on to the star which our model does not address.

As an alternative model, warped and precessing inner disc driven by the radiation pressure in the high X-ray luminosity systems or by the tidal forces caused by the companion could be responsible for the curious torque behaviours (van Kerkwijk et al. 1998; Wijers & Pringle 1999). In this model, torque reversals of 4U 1626–67 were anticipated to occur when the inner disc tilted more than 90° to the unperturbed disc plane. The outer regions of the disc do not necessarily be tilted more than 90° . In other words, the disc is partially counter rotating while its outer part remains prograde. Investigation of the precessing disc and its stability check is beyond our scope in this work. We think that more detailed numerical simulations are requisite in order to favour those kinds of models in addition to more abundant data from the sources experiencing torque reversals.

ACKNOWLEDGEMENTS

The author is grateful to Ü. Ertan for stimulating discussions. The author would like to thank the anonymous referee who provided useful comments helpful for the improvement of the manuscript, D. Altamirano and J. Pétri for useful discussions, İ. Yalçınkaya for his help and suggestions on the figures, and G. Vasilopoulos for comments on the manuscript. The author acknowledges research support from TÜBİTAK (The Scientific and Technological Research Council of Turkey) through the postdoctoral research programme (BİDEB 2219) and CEFIPRA grant IFC/F5904-B/2018.

REFERENCES

- Alpar M. A., Shaham J., 1985, *Nature*, 316, 239
 Archibald A. M. et al., 2015, *ApJ*, 807, 62
 Arons J., 1993, *ApJ*, 408, 160
 Arons J., Lea S. M., 1980, *ApJ*, 235, 1016
 Beri A., Jain C., Paul B., Raichur H., 2014, *MNRAS*, 439, 1940

- Camero-Arranz A., Finger M. H., Ikhsanov N. R., Wilson-Hodge C. A., Beklen E., 2010, *ApJ*, 708, 1500
- Camero-Arranz A., Pottschmidt K., Finger M. H., Ikhsanov N. R., Wilson-Hodge C. A., Marcu D. M., 2012, *A&A*, 546, A40
- Campana S., Gastaldello F., Stella L., Israel G. L., Colpi M., Pizzolato F., Orlandini M., Dal Fiume D., 2001, *ApJ*, 561, 924
- Chakrabarty D., 1998, *ApJ*, 492, 342
- Chakrabarty D. et al., 1997, *ApJ*, 474, 414
- D’Ài A., Cusumano G., Del Santo M., La Parola V., Segreto A., 2017, *MNRAS*, 470, 2457
- Erkut M. H., Alpar M. A., 2004, *ApJ*, 617, 461
- Ertan Ü., 2017, *MNRAS*, 466, 175
- Ertan Ü., 2018, *MNRAS*, 479, L12
- Ertan Ü., Erkut M. H., 2008, *ApJ*, 673, 1062
- Ghosh P., Lamb F. K., 1979, *ApJ*, 234, 296
- Giacconi R., Murray S., Gursky H., Kellogg E., Schreier E., Tananbaum H., 1972, *ApJ*, 178, 281
- Illarionov A. F., Sunyaev R. A., 1975, *A&A*, 39, 185
- Iwakiri W. B. et al., 2019, *ApJ*, 878, 121
- Jetzer P., Strässle M., Straumann N., 1998, *New Astron.*, 3, 619
- Koliopanos F., Gilfanov M., 2016, *MNRAS*, 456, 3535
- Krauss M. I., Schulz N. S., Chakrabarty D., Juett A. M., Cottam J., 2007, *ApJ*, 660, 605
- Levine A., Ma C. P., McClintock J., Rappaport S., van der Klis M., Verbunt F., 1988, *ApJ*, 327, 732
- Makishima K. et al., 1988, *Nature*, 333, 746
- McClintock J. E., Bradt H. V., Doxsey R. E., Jernigan J. G., Canizares C. R., Hiltner W. A., 1977, *Nature*, 270, 320
- Middleditch J., Mason K. O., Nelson J. E., White N. E., 1981, *ApJ*, 244, 1001
- Nelson R. W. et al., 1997, *ApJ*, 488, L117
- Orlandini M. et al., 1998, *ApJ*, 500, L163
- Papitto A., Torres D. F., 2015, *ApJ*, 807, 33
- Parfrey K., Spitkovsky A., Beloborodov A. M., 2016, *ApJ*, 822, 33
- Perna R., Bozzo E., Stella L., 2006, *ApJ*, 639, 363
- Pringle J. E., Rees M. J., 1972, *A&A*, 21, 1
- Raman G., Paul B., Bhattacharya D., Mohan V., 2016, *MNRAS*, 458, 1302
- Rappaport S., Joss P. C., 1977, *Nature*, 266, 683
- Rappaport S. A., Fregeau J. M., Spruit H., 2004, *ApJ*, 606, 436
- Rappaport S., Markert T., Li F. K., Clark G. W., Jernigan J. G., McClintock J. E., 1977, *ApJ*, 217, L29
- Schulz N. S., Chakrabarty D., Marshall H. L., Canizares C. R., Lee J. C., Houck J., 2001, *ApJ*, 563, 941
- Takagi T., Mihara T., Sugizaki M., Makishima K., Morii M., 2016, *PASJ*, 68, S13
- Türkoğlu M. M., Özşükan G., Erkut M. H., Ekşi K. Y., 2017, *MNRAS*, 471, 422
- van Kerkwijk M. H., Chakrabarty D., Pringle J. E., Wijers R. A. M. J., 1998, *ApJ*, 499, L27
- Vasilopoulos G., Lander S. K., Koliopanos F., Bailyn C. D., 2020, *MNRAS*, 491, 4949
- Vaughan B. A., Kitamoto S., 1997, preprint ([arXiv:astro-ph/9707105](https://arxiv.org/abs/astro-ph/9707105))
- Wang Y. M., 1995, *ApJ*, 449, L153
- Wijers R. A. M. J., Pringle J. E., 1999, *MNRAS*, 308, 207

This paper has been typeset from a $\text{\TeX}/\text{\LaTeX}$ file prepared by the author.